

Spectroscopy of $\text{UO}_2\text{Cl}_4^{2-}$ in Basic Aluminum Chloride–1-Ethyl-3-methylimidazolium Chloride

Todd A. Hopkins,[†] John M. Berg,[‡] David A. Costa,[‡] Wayne H. Smith,[‡] and Harry J. Dewey*

Los Alamos National Laboratory, Los Alamos, New Mexico 87545

Received September 8, 2000

The optical absorption, emission, FT Raman, one-photon excitation, two-photon excitation, and luminescence lifetime measurements are reported for $\text{UO}_2\text{Cl}_4^{2-}$ in 40:60 AlCl_3 –EMIC (where EMIC \equiv 1-ethyl-3-methylimidazolium chloride), a room-temperature ionic liquid. Comparison of the spectra with previous results from single crystals containing $\text{UO}_2\text{Cl}_4^{2-}$ allowed the characterization of four ground-state vibrational frequencies, two excited-state vibrational frequencies, and the location of eight electronic excited-state energy levels. The vibrational frequencies and electronic energy levels are found to be consistent with the $\text{UO}_2\text{Cl}_4^{2-}$ ion. Comparison of the one-photon and two-photon excitation spectra, and the relative intensities of the transitions in the emission spectrum indicate that the center of symmetry is perturbed by an interaction with the solvent.

Introduction

Optical spectroscopic techniques are among the most commonly used methods to detect and characterize the uranyl ion, UO_2^{2+} . A characteristic strong green fluorescence allows uranyl to be detected at quite low concentrations in environments where quenching is not prohibitive. Both the fluorescence spectra and the absorption spectra in the blue and ultraviolet are sensitive to the coordination environment of the ion and are used to study uranyl chemistry in solution and solid materials.

Because detailed relationships between optical spectra and molecular structure are not well understood, using the spectra to help determine the stoichiometry and structure of the ion in unknown coordination environments relies on highly empirical comparisons with spectra of compounds of known structure. This usually limits studies to coordination environments that are expected to be similar to structurally characterized crystalline solids.

Aqueous solutions are particularly difficult media in which to study uranyl chemistry because water is a good complexant that competes with other ligands. Most aqueous studies involve sorting out the spectra of multiple mixed-ligand complexes. It is nearly impossible to adjust the conditions so that most of the uranyl ions are in the same chemical form. Complexed water molecules also often lead to significant quenching of the uranyl fluorescence. Solvents in which the chemistry and coordination environment are simplified could provide fruitful media in which to study the relationships between structure and spectroscopy of the uranyl ion.

Room-temperature ionic liquids are a new class of solvents in which the chemistry and coordination environment of the uranyl ion might be significantly simpler than in aqueous systems. These solvents have attracted interest recently because of their potential applications in green chemistry, clean technology development,¹ and nuclear fuel reprocessing.² Because of their low vapor pressure, adjustable acid/base properties, and lack of hydrolysis reactions, room-temperature ionic liquids have

potential as alternative solvents in the separation and purification of actinides. These solvents allow more precise control over both actinide oxidation state and complexation than is possible in aqueous solution. Spectroscopic studies of the uranyl ion in these media are thus of practical interest as characterization tools for future chemical processes and of fundamental interest because coordination environments might be controlled to gain new insights into structure/spectra relationships.

Mixtures of aluminum chloride (AlCl_3) and 1-ethyl-3-methylimidazolium chloride (EMIC) form room-temperature ionic liquids with Lewis acid/base properties that can be adjusted simply by varying the composition of the mixture. Mixtures with >50 mol % of AlCl_3 are Lewis acidic, and mixtures with <50 mol % of AlCl_3 are Lewis basic. Previous studies have examined the chemistry, electrochemistry, and spectroscopy of uranyl and uranium(IV) complexes in basic and acidic AlCl_3 –EMIC.^{3,4} Basic and acidic mixtures of AlCl_3 –EMIC form glasses at low temperature,⁵ providing an excellent medium for low-temperature spectroscopic studies.

Comparison with single-crystal spectra for which detailed assignments are available is usually the most promising way of assigning solution spectra. In an initial study, Dai and co-workers reported the room-temperature absorption spectrum of $\text{UO}_2\text{Cl}_4^{2-}$ in 48:52 AlCl_3 –EMIC⁶ and compared it with the spectrum of $\text{UO}_2\text{Cl}_4^{2-}$ doped in single crystals. They observed subtle differences in relative intensities of broad, adjacent peaks and ascribed them to differences in hydrogen bonding between the solvent and the uranyl ion. However, no explicit assignments of the observed transitions were attempted, either directly or

- (1) Freemantle, M. *Chem. Eng. News* **1998**, 76, 32–37.
- (2) Fields, M.; Hutson, G. V.; Seddon, K. R.; Gordon, C. M. *Ionic Liquids as Solvents*. International Patent WO9806106, Feb 12, 1998.
- (3) Anderson, C. J.; Deakin, M. R.; Choppin, G. R.; D'Olieslager, W.; Heerman, L. *Inorg. Chem.* **1991**, 30, 4013–4016.
- (4) Anderson, C. J.; Choppin, G. R.; Pruet, D. J.; Costa, D.; Smith, W. *Radiochim. Acta* **1999**, 84, 31–36.
- (5) Fannin, A. A.; Floreani, D. A.; King, L. A.; Landers, J. S.; Piersma, B. J.; Stech, D. J.; Vaughn, R. L.; Wilkes, J. S.; Williams, J. L. *J. Phys. Chem.* **1984**, 88, 2614–2621.
- (6) Dai, S.; Shin, Y. S.; Toth, L. M.; Barnes, C. E. *Inorg. Chem.* **1997**, 36, 4900–4902.

* To whom correspondence should be addressed. MS G740.

[†] MS J586.

[‡] MS E505.

by comparison with the crystal spectra. This would have required, at a minimum, obtaining spectra at lower temperatures to attempt to reduce the vibronic complexity and resolve individual transitions.

Single-crystal samples containing the UO₂Cl₄²⁻ ion at temperatures below 10 K have been perhaps the most thoroughly characterized spectra of any uranyl system. Several detailed studies using absorption,⁷ emission,^{8–11} and two-photon excitation¹² techniques have been published. Studies of Cs₂UO₂Cl₄ by Denning and co-workers^{7,12} present an excellent example of the insights into electronic and vibronic structure that can be achieved by applying multiple spectroscopic techniques with polarization control to oriented single crystals.

The spectra of Cs₂UO₂Cl₄ have been analyzed in terms of a $D_{\infty h}$ basis, as is common for discussions of the electronic states of the uranyl ion. The four equatorial chloride ligands lower the symmetry to D_{4h} , which is treated as a perturbation on the states in the $D_{\infty h}$ basis. The UO₂Cl₄²⁻ electronic excited states, over the 20000–33000 cm⁻¹ energy range, derive their principle parentage from the $\sigma_u\delta_u$ and $\sigma_u\phi_u$ electronic configurations of UO₂²⁺ ($D_{\infty h}$).¹² The ground state of UO₂²⁺ is a closed shell of even parity (Σ_g^+ in $D_{\infty h}$), where the highest occupied molecular orbital (HOMO) is a filled, primarily O²⁻-centered σ_u bonding orbital, and the lowest unoccupied molecular orbitals (LUMO) are the U⁶⁺-centered nonbonding $5f_\delta$ and $5f_\phi$ orbitals. Thus, the electronic transitions observed by Denning and co-workers^{7,12} are dominated by parity-conserving (gerade \rightarrow gerade) transitions between the HOMO and LUMO. Electronic transitions to the antibonding $5f_{\pi,\sigma}$ and $6d_{\delta,\pi,\sigma}$ orbitals are higher in energy (>33000 cm⁻¹) and were not observed in these spectroscopic studies.¹³

The electric-dipole selection rules in a centrosymmetric system are primarily dictated by the parity of the initial and final states. One-photon transitions between electronic states of the type gerade \leftrightarrow ungerade are electric-dipole-allowed, while transitions of the type gerade \leftrightarrow gerade are forbidden. In the one-photon absorption (OPA) spectra (below 33 000 cm⁻¹) of UO₂Cl₄²⁻ in Cs₂UO₂Cl₄, where the symmetry is approximately D_{4h} , the electronic transitions observed are derived from either a vibronically induced electric-dipole or magnetic-dipole mechanism.⁷ The vibronically induced electric dipole transitions are displaced from the zero-phonon electronic transitions by the frequency of the enabling ungerade vibrational mode. The one-photon spectra also show vibronic progressions of vibrational quanta of the OUO symmetric stretch (ν_1) built upon the zero-phonon electronic transitions and vibronically induced electric-dipole transitions. Even at 4.2 K, the absorption spectrum is extremely complex because of a large number of possible transitions and was only successfully analyzed and characterized with the aid of the Zeeman effect and polarized spectroscopic measurements.⁷

In two-photon processes (centrosymmetric system), the electric-dipole selection rules for gerade \leftrightarrow gerade electronic transitions are complementary to those operating in one-photon

spectroscopy.¹³ Transitions between electronic states are electric-dipole-allowed in the two-photon excitation (TPE) spectra, and vibronically induced electric-dipole transitions are enabled by gerade vibrational modes. Electronic transitions and their vibronic progressions in ν_1 dominate the observed TPE spectrum of UO₂Cl₄²⁻.¹² Using a combination of low-temperature (4.2 K) polarized OPA and TPE measurements, Denning and co-workers were able to identify and assign 14 excited-state electronic energy levels and numerous excited-state vibrational frequencies of UO₂Cl₄²⁻ in Cs₂UO₂Cl₄ single crystals.

The luminescence spectrum of Cs₂UO₂Cl₄ has also been studied and characterized.⁸ The observed luminescence is derived from a magnetic-dipole allowed electronic transition, vibronically induced electric-dipole transitions, and their vibronic progressions in ν_1 . The vibronically induced transitions in the luminescence spectrum are enabled by the ν_2 (OUO asymmetric stretch), ν_3 (OUO bend), and ν_{10} (OUCl bend) vibrational modes of UO₂Cl₄²⁻. Low-temperature (20 K) polarized luminescence spectra confirmed the assignment (E_g in D_{4h}) for the first excited-state electronic energy level (emitting state) and allowed for the determination of the ground-state vibrational frequencies of ν_1 , ν_2 , ν_3 , and ν_{10} . The luminescence spectra and ground-state vibrational frequencies of UO₂Cl₄²⁻ have also been measured and analyzed for single crystals of [(C₂H₅)₃NH]₂UO₂Cl₄¹⁰ and UO₂Cl₄²⁻ doped in Cs₂ZrCl₆,^{9,11}

No solution system is likely to be as well understood as these crystalline systems, in part because the chromophores in solution cannot be oriented for polarized studies. However, room-temperature ionic liquids are promising solvents for more detailed studies than have usually been applied to uranyl in solution. In this paper we present and discuss absorption, emission, excitation, two-photon excitation, Fourier transform Raman, and time-resolved emission spectra of uranyl (presumed throughout this paper to be UO₂Cl₄²⁻) in 40:60 AlCl₃–EMIC. Direct comparisons to low-temperature crystal results help provide insight into the coordination environment of uranyl in this room-temperature ionic liquid and into the suitability of the solvent for further chemical and spectroscopic studies of actinide complexes.

Experimental Section

Sample Preparation. EMIC was prepared with the method of Smith.¹⁴ AlCl₃ (Aldrich) was purified by sublimation. Ionic liquid preparations were performed in a Vacuum Atmospheres Co. drybox under a He atmosphere. Solutions of UO₂Cl₄²⁻ were prepared by dissolving UO₂Cl₂·2THF in ionic liquids consisting of 40 mol % AlCl₃ and 60 mol % EMIC. Samples were allowed to equilibrate for several hours after preparation before spectroscopic measurements were conducted. Most of the spectroscopic measurements (except the FT Raman) were carried out on samples contained in a 1 cm cuvette. Sample temperatures of 75 K were achieved by suspending the sample cuvette in a liquid nitrogen immersion Dewar. At 75 K, the samples formed frozen glasses of moderate to poor optical clarity with a significant number of cracks in the glass. Samples were often thawed and refrozen to ensure this level of optical clarity.

Emission, Excitation, and Luminescence Lifetime Measurements. The 298 K emission spectra and the 75 K emission and excitation spectra were carried out using a Spex Fluorolog-2 spectrofluorometer and an Aminco-Bowman series 2 spectrofluorometer. Luminescence lifetimes were measured using the Spex Fluorolog-2 with the 1943D phosphorimeter accessory. The excitation spectra were measured over the 400–515 nm wavelength range, monitoring the emission intensity

- (7) Denning, R. G.; Snellgrove, T. R.; Woodwark, D. R. *Mol. Phys.* **1976**, *32*, 419–442.
- (8) Flint, C. D.; Tanner, P. A. *J. Chem. Soc., Faraday Trans. II* **1978**, *74*, 2210–2217.
- (9) Flint, C. D.; Tanner, P. A. *J. Lumin.* **1979**, *18–9*, 69–72.
- (10) Flint, C. D.; Tanner, P. A. *J. Chem. Soc., Faraday Trans. II* **1979**, *75*, 1168–1178.
- (11) Metcalf, D. H.; Dai, S.; Delcul, G. D.; Toth, L. M. *Inorg. Chem.* **1995**, *34*, 5573–5577.
- (12) Barker, T. J.; Denning, R. G.; Thorne, J. R. G. *Inorg. Chem.* **1987**, *26*, 1721–1732.
- (13) Denning, R. G. *Struct. Bonding* **1992**, *79*, 215–276.

- (14) Smith, G. P.; Dworkin, A. S.; Pagni, R. M.; Zingg, S. P. *J. Am. Chem. Soc.* **1989**, *111*, 525.

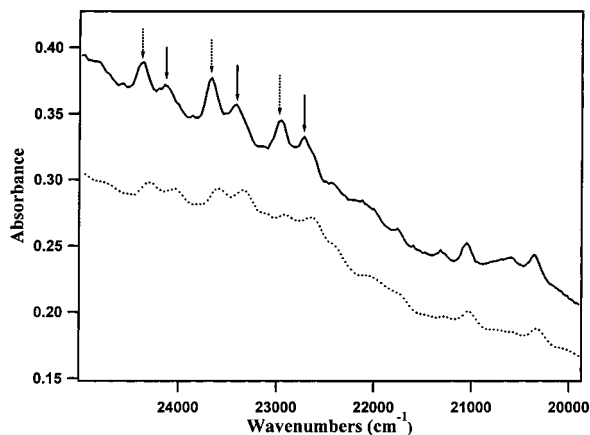


Figure 1. Absorption spectra of $\text{UO}_2\text{Cl}_4^{2-}$ in 40:60 AlCl_3 -EMIC at 298 K (dotted line) and 75 K (solid line).

at 525 nm. The emission and luminescence lifetimes were measured using variable excitation wavelengths.

Absorption. The 298 and 75 K absorption measurements were carried out using a Perkin-Elmer Lambda 19 UV-vis-NIR spectrometer. The absorption spectra were measured over the 350–1500 nm wavelength range.

Two-Photon Excitation. The excitation source was a Nd:YAG (Continuum Powerlite 8000) laser pumping a tunable optical parametric oscillator (Continuum Mirage 500) laser operating at a 10 Hz repetition rate. Pulse energies were typically 4–9 mJ over the 720–1005 nm excitation-wavelength range. The excitation beam was passed through a red-blocking long-pass filter and nominally was focused ca. 3–5 cm beyond the sample. The emission was detected at a 90° angle to the excitation through a band-pass filter with a fwhm bandwidth of 12 nm centered at 547.5 nm. The emission intensity was measured using a Hamamatsu photomultiplier tube (model no. R928), SR445 preamplifier, and a SR400 gated photon counter. The luminescence intensity was measured by collecting photon counts for 4 ms (ca. 2 luminescence lifetimes), beginning 30 μs after the laser pulse to avoid rf interference. The background intensity (noise and dark counts) was measured by collecting photon counts for 4 ms, beginning 12 ms after the excitation pulse. Typically, the photon counts were summed over 20 laser pulses and stored on a computer interfaced to the photon counter. Laser pulse intensities were monitored using a silicon photodiode detector over the entire excitation wavelength range. The background counts were subtracted from the luminescence intensity and scaled by the average of the square of the photodiode output of the last 10 (out of 20) laser pulses. Sample scattering considerably distorted the focus, so the true beam profile within the sample is unknown and variable with slight changes in alignment. This makes normalization attempts of questionable value for comparing intensities over widely separated wavelengths. No attempt was made to eliminate (or account for) the effects of pulse-to-pulse fluctuations in the laser intensity more rapid than the 10-pulse average.

FT Raman. Fourier transform Raman spectra were collected on a Nicolet Raman 960 ESP attachment to the Magna-IR 560 FT-IR spectrometer using an InGaAs detector. The sample was irradiated with ~ 0.5 W from an air-cooled diode-pumped Nd:YVO₄ CW laser operating at 1064 nm, and the scattered light was collected with 180° collection optics and relayed to the FT-IR interferometer. Spectra were collected at 4 cm^{-1} resolution and signal-averaged over 2048–4096 scans. All of the FT Raman measurements were conducted on samples at 298 K.

Results and Discussion

Absorption Spectra. Figure 1 shows the 298 K (dotted line) and 75 K (solid line) absorption spectra of $\text{UO}_2\text{Cl}_4^{2-}$ in 40:60 AlCl_3 -EMIC measured over the 19700–25000 cm^{-1} (400–510 nm) energy range. This spectroscopic region has been shown to encompass transitions from the ground state to the

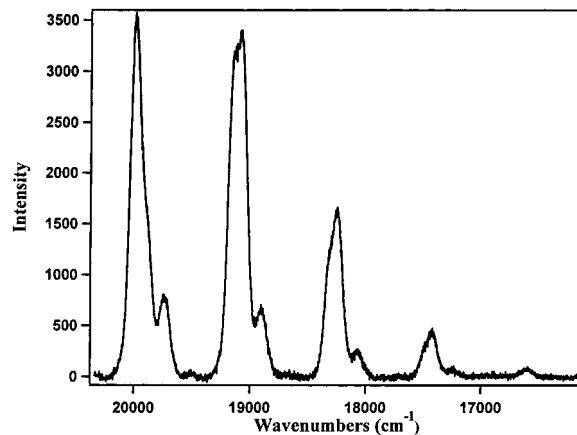


Figure 2. Emission spectrum of $\text{UO}_2\text{Cl}_4^{2-}$ in 40:60 AlCl_3 -EMIC at 75 K. The intensity scale is given in arbitrary units.

eight lowest-energy electronic excited states of $\text{UO}_2\text{Cl}_4^{2-}$ and numerous vibronically induced transitions in low-temperature single crystals of $\text{Cs}_2\text{UO}_2\text{Cl}_4$.⁷ Polarized-absorption and Zeeman effect measurements were required to make definitive assignments of the electronic and vibronic states.⁷ These techniques are not useful for our samples. The absorption spectra in Figure 1 show background absorbances that obscure many of the spectral features of the $\text{UO}_2\text{Cl}_4^{2-}$ ion. The complexity of the electronic and vibronic structure of $\text{UO}_2\text{Cl}_4^{2-}$, the breadth of the peaks, and the lack of uniform macroscopic orientation of the chromophores make it impossible to analyze these spectra with anything approaching the rigor that has been applied to crystalline systems. However, we can take advantage of the work on single crystals by comparing our spectra to those and proposing assignments by equating transitions that have the same spectroscopic properties.

In the frozen glass absorption spectra, the two groups of three peaks, denoted by solid- and dotted-line arrows, are vibronic progressions in the UO_2^{2+} symmetric stretching (ν_1) mode based on electronic or vibronically induced origins. The excited-state frequency of ν_1 , determined from the data in Figure 1, is 710 cm^{-1} . To within the precision of our measurement, this is identical to the frequency of ν_1 (711 cm^{-1}) found in $\text{Cs}_2\text{UO}_2\text{Cl}_4$.¹² It is also important to note that when the sample is cooled from 298 K (solution) to 75 K (frozen glass), the absorption peaks shift to higher energy because the thermal population of vibronic energy levels in the ground state has changed at low temperature. The two absorption spectra shown in Figure 1 show no major changes in the overall peak structure or relative intensities, and this indicates that there are no significant structural changes in the $\text{UO}_2\text{Cl}_4^{2-}$ ion (the chromophore) between solution and frozen glass in 40:60 AlCl_3 -EMIC.

Dai and co-workers have previously reported the room-temperature absorption spectrum of $\text{UO}_2\text{Cl}_4^{2-}$ in 48:52 AlCl_3 -EMIC (also a Lewis base).⁶ Examination of the 298 K absorption spectrum in Figure 1 shows that the peak locations are identical to those found by Dai et al. They argued that the relative intensities of the peaks are directly related to a hydrogen-bonding interaction between the uranyl (U–O) of $\text{UO}_2\text{Cl}_4^{2-}$ and a hydrogen atom on the imidazolium ring in EMIC. However, because the spectral features in Figure 1 (298 K) are relatively broad and unresolved, it is difficult to make more than a qualitative comparison between our results and theirs.

Emission Spectra. The 75 K emission spectrum of $\text{UO}_2\text{Cl}_4^{2-}$ in 40:60 AlCl_3 -EMIC is shown in Figure 2. The 20500–16000 cm^{-1} energy range encompasses the magnetic-dipole-allowed electronic (origin) transition $A_{1g} \leftarrow E_g$ (in D_{4h} symmetry),⁸ the

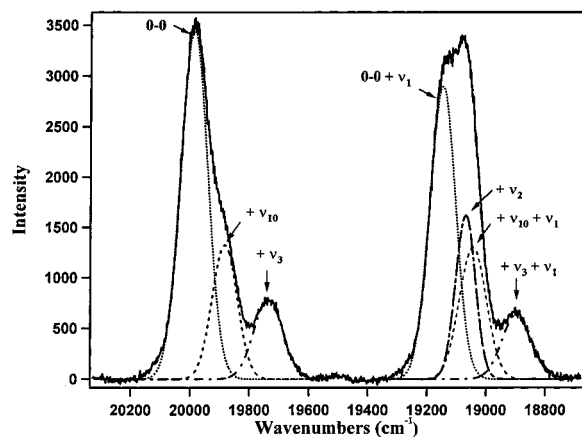


Figure 3. Gaussian fits to the electronic origin (···) and the vibronic bands based on the ν_2 (—), ν_3 (---), and the ν_{10} (---) of the first two members of the progression in ν_1 of the emission spectrum (solid line) of UO₂Cl₄²⁻ in 40:60 AlCl₃–EMIC at 75 K. The intensity scale is given in arbitrary units.

vibronically induced electric-dipole transitions enabled by three ungerade vibrational modes, and the first four members of a vibronic progression in ν_1 . Metcalf and coauthors have reported the emission spectra of UO₂Cl₄²⁻ doped in Cs₂ZrCl₆ single-crystal samples over the 20–125 K temperature range.¹¹ Comparison of the spectrum in Figure 2 with the 75 K spectrum reported by Metcalf et al. shows that the observed transition line widths are significantly broader than in the single-crystal spectrum.

Because of the broad line widths, several of these transitions and their progressions in ν_1 shown in Figure 2 are not well resolved. Therefore, the ground-state vibrational frequencies for UO₂Cl₄²⁻ in 40:60 AlCl₃–EMIC were determined by fitting the emission data to a set of Gaussians representing the electronic and vibronic transitions. Following an initial subtraction of a broad background, the minimum was determined using a Levenberg–Marquardt nonlinear least-squares fitting algorithm. Fits to the electronic origin, the vibronically induced transitions derived from the ν_2 (O–U–O asymmetric stretch), ν_3 (O–U–O bend), and ν_{10} (O–U–Cl bend) ungerade vibrational modes, and their vibronic progressions in ν_1 provided excellent agreement with the experimental emission data. The emission data and the results of Gaussian fits to that data over the 18750–20400 cm⁻¹ energy region (the first two members of the vibronic progression) are shown in Figure 3. No significant improvements of the fits were obtained by including additional ungerade vibrational modes. The very weak feature located at 19575 cm⁻¹, which could be due to combination vibrational modes or solvent modes, was left unassigned.

Table 1 shows the vibrational frequencies determined from these fits along with frequencies previously reported for single crystals containing UO₂Cl₄²⁻. The vibrational frequencies determined for UO₂Cl₄²⁻ in 40:60 AlCl₃–EMIC are remarkably similar to the results determined from single-crystal samples. The vibrational frequency of 241 cm⁻¹ in the present study is assigned to the ν_3 mode according to the notation of Denning.⁷ There is some ambiguity in the assignment of the ν_3 and ν_6 vibrational modes in the literature,⁸ but there is likely to be a significant amount of mixing of these modes. Where only one of these modes (ν_3 or ν_6) is experimentally determined, the frequency is assigned to ν_3 in Table 1.

The relative intensity of the zero-phonon origin ($A_{1g} \leftarrow E_g$) transition to the vibronically induced transitions in the emission spectrum can be used to indicate a deviation from a center of

symmetry of the UO₂²⁺ ion. A noncentrosymmetric environment allows the origin transition to acquire electric-dipole intensity that gives it a greater relative intensity with respect to the vibronically induced transitions. In UO₂Cl₄²⁻-doped Cs₂SnCl₆ single crystals, where the center of symmetry is perturbed by the crystalline environment, the relative intensity of the origin transition is larger than that found in the emission of Cs₂UO₂Cl₄ crystals, a centrosymmetric environment.⁹ The relative intensity of the origin transition of UO₂Cl₄²⁻ in 40:60 AlCl₃–EMIC is also much larger than that found in Cs₂UO₂Cl₄, indicating that the environment of the uranyl ion in this room-temperature ionic liquid is also not rigorously centrosymmetric.

A single-exponential decay with a lifetime of 1.6 ms was observed in the time-resolved luminescence of samples of UO₂Cl₄²⁻ in 40:60 AlCl₃–EMIC at 75 K. For comparison, the lifetimes of UO₂Cl₄²⁻ in cubic single crystals are 870 μ s at 300 K¹⁵ and 3.2 ms at 80 K.⁹

FT Raman Spectra. The vibrational frequency of ν_1 (838 \pm 6 cm⁻¹) determined from the 75 K emission measurements is in good agreement with previous crystal studies (Table 1), though the uncertainty is large because of the large line widths. A more precise ν_1 frequency may be obtained from Raman measurements. FT Raman measurements were recorded for samples of UO₂Cl₄²⁻ in 40:60 AlCl₃–EMIC at 298 K over the 100–3500 cm⁻¹ energy range. Over this energy range the spectrum is dominated by a large number of Raman-active vibrational modes of the solvent (AlCl₃–EMIC). The solvent modes hide most of the vibrational modes of the UO₂Cl₄²⁻, but a signal is detected at 832 cm⁻¹, the frequency of the ν_1 (OUO symmetric stretch) mode. This is in good agreement with the results from Cs₂UO₂Cl₄ crystals.

Excitation Spectra. As described above, the low-temperature absorption spectra shown in Figure 1 have significant background absorbances, which obscure many of the UO₂Cl₄²⁻ electronic and vibronic transitions. Emission-detected excitation spectroscopic techniques can provide similar information about the UO₂Cl₄²⁻ ion as absorption spectra while eliminating background interference due to the solvent and impurities (which do not emit at the detection wavelength). The 75 K excitation spectrum of UO₂Cl₄²⁻ in 40:60 AlCl₃–EMIC is shown in Figure 4. The excitation spectrum eliminates the baseline interference, but is otherwise not notably different from the absorption spectra in Figure 1, with respect to the location and relative intensities of the UO₂Cl₄²⁻ transitions. As previously discussed, this region of the spectrum is extremely complex with a relatively high density of states (electronic and vibronic). Without the use of polarized spectroscopic techniques on oriented chromophores, it is difficult to make an independent assignment of the transitions. Additionally, the broad line widths of the transitions make it difficult to compare the spectrum in Figure 4 with previous single-crystal absorption measurements of UO₂Cl₄²⁻.^{7,10} We will return to a discussion of the excitation spectrum following the discussion of the two-photon excitation spectra presented below.

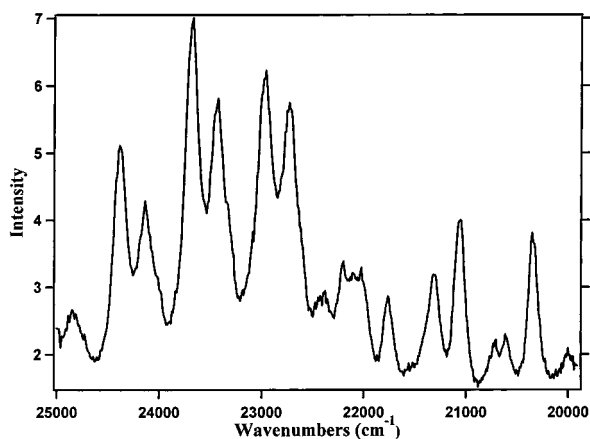
Two-Photon Excitation Spectra. One-photon excitation and absorption spectra of transitions between electronic states of the same parity in centrosymmetric systems are complex and congested because they are dominated by vibronic bands. The pure electronic transitions are electric-dipole-forbidden in the absence of a noncentrosymmetric perturbation, whereas vibronic transitions that excite odd-parity vibrational modes in addition to the electronic excited state can be dipole-allowed. Because

(15) Tanner, P. A.; Dexpertghys, J.; Pei, Z. W.; Lin, J. *Chem. Phys.* **1997**, 215, 125–130.

Table 1. Comparison of Ground-State Vibrational Frequencies (cm^{-1}) Determined from the Luminescence Spectra of $\text{UO}_2\text{Cl}_4^{2-}$ in 40:60 AlCl_3 -EMIC and Several Crystalline Hosts

mode ^a	symmetry ^a	$\text{Cs}_2\text{UO}_2\text{Cl}_4$ ^b	$\text{Cs}_2\text{ZrCl}_6/\text{UO}_2\text{Cl}_4^{2-}$ ^c	$\text{Cs}_2\text{SnCl}_6/\text{UO}_2\text{Cl}_4^{2-}$ ^d	$[(\text{Et})_3\text{NH}]_2\text{UO}_2\text{Cl}_4$ ^e	$\text{UO}_2\text{Cl}_4^{2-}$ in basic AlCl_3 -EMIC ^f
ν_1	a_{1g}	836	819	820	841	838(6)
ν_2	a_{2u}	916	901	901	921	907(5)
ν_3	e_u	246	247	251	239/245	241(9)
ν_4	a_{1g}			279	259	
ν_6	e_u				259/265	
ν_{10}	b_{1u}	108	116	113	83	107(6)

^a The notation of Denning⁷ has been used to describe the normal modes in D_{4h} symmetry. ^b From ref 8. ^c From ref 11. ^d From ref 9. ^e From ref 10. ^f Determined using Gaussian fits to the emission data. The uncertainties are shown in parentheses.

**Figure 4.** Excitation spectrum of $\text{UO}_2\text{Cl}_4^{2-}$ in 40:60 AlCl_3 -EMIC at 75 K. The intensity scale is given in arbitrary units.

there are many more vibronic transitions than electronic transitions, this adds complexity to the spectra.

Two-photon transitions, in contrast, are allowed by electric-dipole mechanisms between states of the same parity. Pure electronic transitions are expected to be significantly stronger than most vibronic transitions in TPE spectra. This leads to simpler spectra that can be significantly easier to assign. Two-photon excitation spectra played a significant role in the most detailed characterization of the electronic (and vibronic) structure of $\text{UO}_2\text{Cl}_4^{2-}$ in $\text{Cs}_2\text{UO}_2\text{Cl}_4$,¹² augmenting the one-photon spectra.⁷ We use the results from those studies to analyze the TPE and one-photon excitation (OPE) spectra of the $\text{UO}_2\text{Cl}_4^{2-}$ ion in 40:60 AlCl_3 -EMIC.

The 75 K TPE spectrum (solid line) of $\text{UO}_2\text{Cl}_4^{2-}$ in 40:60 AlCl_3 -EMIC is shown in Figure 5, with the 75 K OPE spectrum (dotted line) included for comparison purposes. Of the 18 prominent features, comparison with the $\text{Cs}_2\text{UO}_2\text{Cl}_4$ studies¹² suggests that 17 can be attributed to 8 electronic energy levels of $\text{UO}_2\text{Cl}_4^{2-}$ and their progressions in ν_1 . The labels shown in Figure 5 denote the assignment of these transitions based upon this comparison. The labeling scheme is identical to that of Denning.^{7,12} Table 2 contains a summary of the assigned electronic energy levels.

The irreducible representation labels in Table 2 are presented for D_{4h} site symmetry. Both D_{4h} and D_{2h} point group irreducible representations have been used in previous studies to describe the symmetry of the electronic states of the $\text{UO}_2\text{Cl}_4^{2-}$ ion. The single-crystal X-ray structure of $\text{Cs}_2\text{UO}_2\text{Cl}_4$ showed the site symmetry of the uranium atoms to be C_{2h} , but the distortion from D_{2h} is small.^{12,16} Most of the features of the single-crystal spectra have been explained using D_{4h} symmetry because even the distortion from D_{4h} produces small or negligible effects.

Observed splittings of the E_g states by 1 and 50 cm^{-1} were explained by including a perturbation that reduces the symmetry to D_{2h} , where each E_g state is split into two singly degenerate energy levels (B_{2g} and B_{3g}). Similar splitting of these states in 40:60 AlCl_3 -EMIC would not be evident in the spectra because the peaks are much broader than in the crystal. Since 17 out of 18 transitions correlate with electronic and vibronic transitions observed in $\text{Cs}_2\text{UO}_2\text{Cl}_4$ using the D_{4h} assignments, it is unlikely that the actual symmetry of $\text{UO}_2\text{Cl}_4^{2-}$ in 40:60 AlCl_3 -EMIC deviates significantly from D_{4h} .

In $\text{Cs}_2\text{UO}_2\text{Cl}_4$, the transition lines found in the TPE spectra exhibit homogeneous widths that are typically $\sim 1 \text{ cm}^{-1}$ and are significantly narrower than lines from the OPA spectra.¹² As shown in Figure 5, the transition lines for the TPE spectra in 40:60 AlCl_3 -EMIC are much broader ($\sim 70 \text{ cm}^{-1}$) than in the single crystal, and there is no significant difference in line width between the OPE and TPE spectra. The differences in line widths for ionic liquid vs single-crystal results are consistent with inhomogeneous line broadening due to the solvation environment of the 40:60 AlCl_3 -EMIC.

Many of the transitions to electronic origins (i.e., III, IV, and VIII) identified in the TPE are also among the most intense spectral features in the OPE spectra. This runs counter to the expectation that pure electronic transitions should be minor or absent in the one-photon spectra. Magnetic-dipole-transition mechanisms can explain some but not all of the peaks. Transitions to III (B_{2g}), IV (B_{1g}), and VIII (B_{2g}) are both electric- and magnetic-dipole-forbidden⁷ in one-photon absorption. Therefore, the transitions to III, IV, and VIII (and possibly other lines) in the OPE spectrum must acquire their intensity from a breakdown in the center of symmetry of the $\text{UO}_2\text{Cl}_4^{2-}$ ion either by a noncentrosymmetric interaction with the solvent or by a vibronic mechanism involving vibrational modes with frequencies comparable to the observed line widths of the transitions.

There are several transitions found in the OPE that are absent in the TPE spectra. Most of these transitions are impossible to identify and are left unassigned. However, three of the most intense OPE transitions can be assigned to the vibronically induced transition, VIII + ν_3 , and its vibronic progression in ν_1 (labels shown in Figure 5). The excited-state vibrational frequency of ν_3 determined from the results in Figure 5 is 241 cm^{-1} . This is identical, within the uncertainty of the experiment, to the ν_3 frequency ($\sim 235 \text{ cm}^{-1}$) determined in $\text{Cs}_2\text{UO}_2\text{Cl}_4$ single-crystal OPE results.⁷

The OPE and TPE results shown in Figure 5 are consistent with a noncentrosymmetric solvent/uranyl ion interaction. The presence of several forbidden electronic transitions in the OPE spectrum and the absence of high-frequency vibronically induced transitions based on ungerade vibrational modes in the TPE spectrum suggest a weak perturbation of the $\text{UO}_2\text{Cl}_4^{2-}$ ion from its ideal geometry. Dai and co-workers have argued that several of the transitions in their room-temperature absorption spectra of $\text{UO}_2\text{Cl}_4^{2-}$ in basic AlCl_3 -EMIC become electric-dipole-

(16) Denning, R. G.; Snellgrove, T. R.; Woodwark, D. R. *Mol. Phys.* **1975**, *30*, 1819.

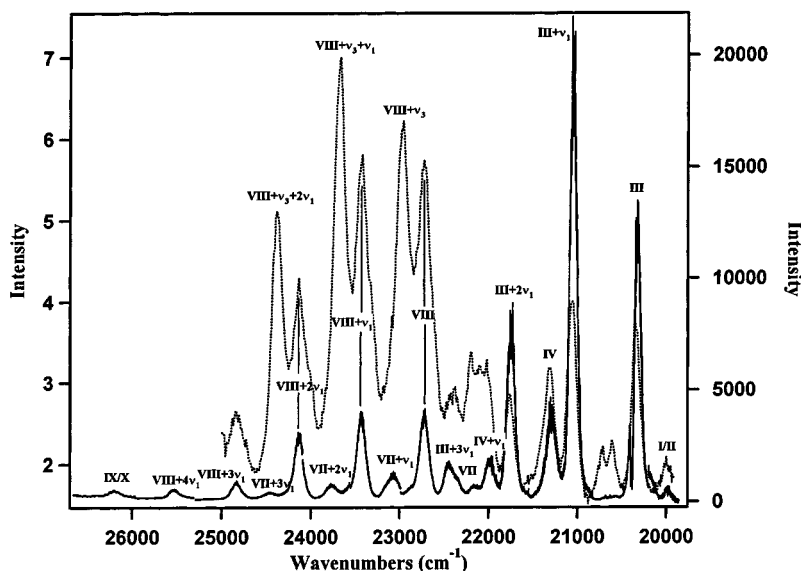


Figure 5. Two-photon excitation (solid line) and excitation spectra (dotted line) UO₂Cl₄²⁻ in 40:60 AlCl₃-EMIC at 75 K. The energy scale for the TPE is 2 times the incident photon energy. The peak-labeling scheme is discussed in the text. The left-hand intensity scale (arbitrary units) corresponds to the OPE spectrum, and the right-hand intensity scale (arbitrary units) corresponds to the TPE spectrum. Discontinuities in the TPE spectrum are due to differences in experimental conditions (optical quality of the frozen glass, laser performance, etc.) between measurements of different spectral regions.

Table 2. Comparison of Electronic Transitions Observed in the Two-Photon Excitation Spectra of UO₂Cl₄²⁻ in 40:60 AlCl₃-EMIC vs Cs₂UO₂Cl₄

origin ^b	Cs ₂ UO ₂ Cl ₄ ^a			UO ₂ Cl ₄ ²⁻	
	symmetry ^b	energy (cm ⁻¹)	ν_1 (cm ⁻¹)	energy ^c (cm ⁻¹)	ν_1 (cm ⁻¹)
I	E _g	20 096	714.8	19 992	
II		20 097	714.6		
III	B _{2g}	20 406	710.3	20 323	725
IV	B _{1g}	21 316	696	21 294	708
V	E _g	22 026	712		
VI		22 076	710		
VII	B _{1g}	22 406	717	22 365	713
VIII	B _{2g}	22 750	711	22 722	715
IX	E _g	26 197	724.7	26 202	
X		26 247	724.3		

^a From ref 12. ^b Origin labels according to the notation of Barker et al. The irreducible representations are given assuming a D_{4h} point group symmetry. However, in Cs₂UO₂Cl₄ the symmetry is strictly D_{2h}, and this has the effect of splitting the E_g states into two singly degenerate energy levels. ^c From present work. The uncertainty in the location of energy levels is ca. 15 cm⁻¹.

allowed via a symmetry distortion induced by uranyl/imidazolium hydrogen-bonding interaction.⁶ Our results are consistent with their argument but are not conclusive because the same data could result from several different perturbation mechanisms.

Spectra/Structure Relationship. To summarize, similarities in the absorption spectra (Figure 1) at 298 and 75 K spectra show that the structure of the uranyl complex is the same in solution and frozen glass. Observation of single-exponential fluorescence decay at 75 K indicates that there is only one emitting uranyl complex. Additionally, fits to the emission spectrum gave ground-state vibrational frequencies that are in good agreement with those found for UO₂Cl₄²⁻ in single crystals.⁸⁻¹¹

The TPE spectrum gives an excited-state electronic structure and (U-O) symmetric stretch frequency that is consistent with UO₂Cl₄²⁻ in D_{4h} point group symmetry.¹² Interpretation of the OPE indicates a small deviation from a center of symmetry, allowing some pure electronic transitions in the OPE spectrum.

The relative intensity of the origin transition compared to the vibronically induced electric dipole transitions in the emission spectrum also indicates a deviation from a center of symmetry. This is likely to be the result of a noncentrosymmetric interaction between the uranyl ion and the AlCl₃-EMIC solvent.

Conclusion

We have presented results from several different spectroscopic techniques conducted on solution and frozen glass (75 K) samples of UO₂Cl₄²⁻ in 40:60 AlCl₃-EMIC. The ground- and excited-state vibrational frequencies and excited-state electronic energy levels determined from our spectroscopic results are remarkably similar to previous results from studies of UO₂Cl₄²⁻ in single crystals. Comparison of the one- and two-photon spectroscopic results shows that the basic AlCl₃-EMIC ionic liquid plays a role in mediating the spectroscopic properties of the UO₂Cl₄²⁻ ion.

Since the optical spectroscopy of the uranyl ion is extremely sensitive to the number and nature of equatorial ligands, the results presented in this paper indicate that UO₂Cl₄²⁻ is the *only* uranyl species present in 40:60 AlCl₃-EMIC. The presence of a single species is quite unusual in a solution system, where the complexation is often complicated by competition between chloride and solvent. Not only does this simple speciation in the ionic liquid allow for characterization of the spectroscopy but it also provides an opportunity to study the chemical properties of UO₂Cl₄²⁻ in solution without interferences from other complexes.

Acknowledgment. This work was supported by the Office of Basic Energy Sciences, Division of Chemical Sciences, U.S. Department of Energy and the Laboratory Directed Research and Development program of the Los Alamos National Laboratory, operated by the University of California under contract to the U.S. Department of Energy. The authors also thank Drew Tait (FT Raman) and Dawn Coffelt (sample preparation).